Physics of the Solid State, Vol. 44, No. 7, 2002, pp. 1339–1344. Translated from Fizika Tverdogo Tela, Vol. 44, No. 7, 2002, pp. 1280–1284.

MAGNETISM AND FERROELECTRICITY

Synthesis of the New Oxocuprate $Cu_5Bi_2B_4O_{14}$ and Investigation of Its Structural, Magnetic, and Resonant Properties

G. A. Petrakovskiĭ*, K. A. Sablina*, A. I. Pankrats*, D. A. Velikanov*, A. D. Balaev*, O. A. Bayukov*, V. I. Tugarinov*, A. M. Vorotynov*, A. D. Vasil'ev*, G. V. Romanenko, and Yu. G. Shvedenkov****

** Kirensky Institute of Physics, Siberian Division, Russian Academy of Sciences, Akademgorodok, Krasnoyarsk, 660036 Russia*

*** Institute of Inorganic Chemistry, Siberian Division, Russian Academy of Sciences, pr. Akademika Lavrent'eva 3, Novosibirsk, 630090 Russia*

e-mail: pank@iph.krasn.ru

Received October 30, 2001

Abstract—Single crystals of the new compound $Cu_5Bi_2B_4O_{14}$ are grown and its structural, magnetic, and resonant properties are investigated for the first time. It is found that the $Cu_5Bi_2B_4O_{14}$ crystal synthesized has a triclinic symmetry with space group $P\bar{1}$ and the unit cell parameters $a = 10.132$ Å, $b = 9.385$ Å, $c = 3.458$ Å, $\alpha = 105.443°$, $\beta = 97.405°$, $\gamma = 107.784°$, and $Z = 1$. At a temperature of 24.5 K, the crystal undergoes a magnetic phase transition to the magnetically ordered state. The assumption is made that the ferrimagnetic structure of the $Cu_5Bi_2B_4O_{14}$ crystal consists of two ferromagnetic sublattices coupled through the antiferromagnetic exchange interaction. The unit cell of the crystal contains five copper ions, of which one ion belongs to the first sublattice and the other four ions form the second sublattice. Analysis of the resonant and magnetic static properties demonstrates that the $Cu_5Bi_2B_4O_{14}$ crystal exhibits an easy-axis magnetic anisotropy. The direction of the easy axis coincides with the *c* axis of the crystal, whereas the *a* and *b* axes are the hard magnetic axes with saturation fields approximately equal to 25 and 10 kOe, respectively. © *2002 MAIK "Nauka/Interperiodica".*

1. INTRODUCTION

The discovery of high-temperature superconductivity gave impetus to active research into oxocuprates. Although oxocuprates possess neither superconductivity nor even metallic conductivity, their crystal structure involves fragments that are similar to those of high-temperature superconductors and determine the magnetic properties of the former compounds in the case of superexchange interactions. In his monograph, Wells [1] noted that bivalent copper should form a larger variety of magnetic structures than is observed for any other chemical element. The great diversity of the magnetic properties of copper oxide compounds can be illustrated using the oxocuprates studied in our earlier works. In particular, $CuGeO_3$ is a chain spin-Peierls magnet with the transition temperature $T_{SP} = 14$ K [2, 3], $LiCu_2O_2$ is a two-dimensional antiferromagnet with a damaged ladder structure and the magnetic phase transition temperature $T_N = 24$ K [4], and Bi_2CuO_4 is a three-dimensional antiferromagnet characterized by the four-spin exchange interaction and the Néel temperature $T_N = 41$ K [5]. For CuB_2O_4 [6–9], the magnetic states at temperatures below 20 K are described by a complex phase diagram, including the transition between the commensurate and incommensurate structures. This paper reports on the first results of investigations into the structural, magnetic, and resonant properties of a new oxocuprate which we found in the ternary $CuO–Bi_2O_3–B_2O_3$ system.

2. GROWTH OF SINGLE CRYSTALS

Earlier, Zargarov *et al.* [10] performed physicochemical investigations into the ternary $CuO–Bi_2O_3–B_2O_3$ system and revealed two copper oxide compounds, namely, $2Bi_2O_3 \cdot CuO \cdot B_2O_3$ and $Bi_2O_3 \cdot 2CuO \cdot B_2O_3$, which crystallize in the orthorhombic crystal system. We also studied the $CuO–Bi_2O_3–B_2O_3$ system and found a new compound with the chemical formula $Cu_5Bi_2B_4O_{14}$.

Single crystals of $Cu_5Bi_2B_4O_{14}$ were grown by spontaneous crystallization from a molten mixture containing 22 mol % Bi_2O_3, 50 mol % CuO, and 28 mol % B_2O_3. Dark green crystals of different shapes were mechanically removed from the crucible. A number of crystals had a perfect faceting typical of bulk skewed prisms, whereas the other crystals had a flatter shape with a less pronounced faceting. Crystals of a particular type could be predominantly grown by varying the ratio of the initial oxides in certain limits. It turned out that crystals of both types exhibited identical x-ray diffraction patterns.

1063-7834/02/4407-1339$22.00

X-ray diffraction analysis was performed both with powders of ground crystals on a DRON-2 diffractometer and with small-sized high-quality single crystals on a CAD4 automated diffractometer (MoK_α radiation). It was found that the crystals synthesized have a triclinic symmetry with space group $P\bar{1}$. The unit cell parameters are as follows: a = 10.132 Å, b = 9.385 Å, c = 3.458 Å, α = 105.443°, β = 97.405°, γ = 107.784°, and Z = 1.

The magnetic susceptibility and the magnetization were measured on a SQUID magnetometer in magnetic fields up to 40 kOe and on a vibrating-coil magnetometer in fields up to 30 kOe in the temperature range 4.2–300 K at different orientations of the magnetic field with respect to the crystallographic axes.

3. EXPERIMENTAL RESULTS

Figure 1 displays the temperature dependences of the magnetic susceptibility and the reciprocal of the magnetic susceptibility for a sample composed of a set of single crystals oriented in a random manner. In the temperature range 170–300 K, the magnetic susceptibility is adequately described by the Curie–Weiss law $\chi = C/(T - \Theta)$ with the following parameters: $C = 2.01 \times 10^{-3}$ K cm^3/g and Θ = +17.4 K. The effective magnetic moment is estimated as $\mu_{eff} = 0.81\mu_B$. Judging from the positive paramagnetic Curie temperature, this compound predominantly undergoes a ferromagnetic exchange interaction, which is rarely observed in oxocuprates [11, 12].

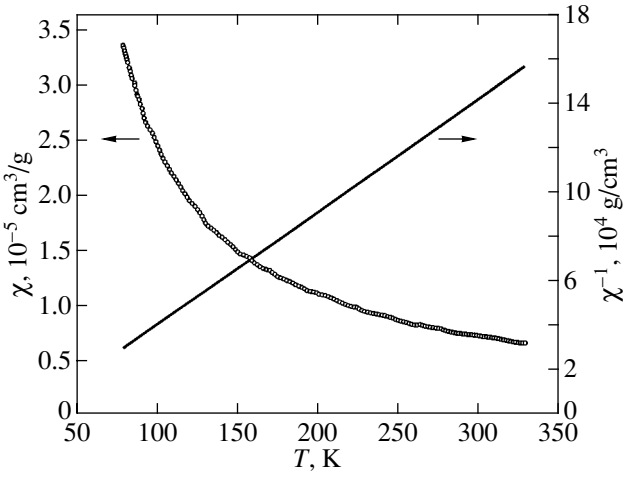

Fig. 1. Temperature dependences of the magnetic susceptibility and the reciprocal of the magnetic susceptibility for the $Cu_5Bi_2B_4O_{14}$ crystal.

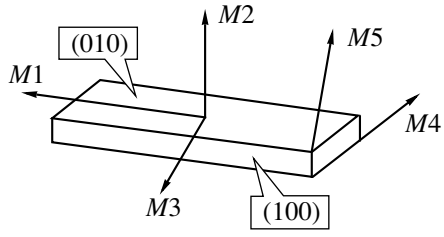

Fig. 2. A geometric shape of the $Cu_5Bi_2B_4O_{14}$ samples and the magnetic field orientations used in the measurements.

The temperature and field dependences of the magnetization of the single crystals under investigation were measured at different magnetic field orientations. Figure 2 shows a geometric shape of the single-crystal samples; in this figure, the magnetic field orientations used in the measurements are designated as $M1$–$M5$. The samples used in these experiments have the form of plates elongated in one direction. The longer edge of the plate is oriented along the c axis of the crystal. The largest and elongated lateral faces lie in the (010) and (100) crystallographic planes, respectively. The magnetic field orientation $M1$ coincides with the c axis of the crystal, the orientation $M2$ is perpendicular to the (010) face, and the field orientation $M3$ is aligned with the (010) plane and is perpendicular to the orientation $M1$. The field orientations $M4$ and $M5$ coincide with the shorter edges of the crystal.

Figure 3 depicts the field dependences of the magnetization measured at T = 5 K. For the field orientations $M1$–$M3$, the magnetization linearly increases to saturation and remains virtually constant with a further increase in the magnetic field strength. The saturation magnetizations at the orientations $M1$ and $M2$ coincide with each other and amount to 17.1 emu/g at T = 5 K. The saturation magnetization at the orientation $M3$ is equal to 16.6 emu/g. The saturation fields at the orientations $M1$, $M2$, and $M3$ are approximately equal to 350 Oe, 8 kOe, and 23 kOe, respectively. The field dependences of the magnetization at the orientations $M4$ and $M5$ exhibit a nonlinear behavior. Since the magnetization directions $M4$ and $M5$ are close to the directions $M3$ and $M2$, respectively, the field dependences of the magnetization for the directions $M4$ and $M5$ are characterized by the saturation fields which are approximately identical to those for the directions $M3$ and $M2$. The specific feature of the field dependences is that they are anhysteretic to within the experimental error of the magnetization measurement.

The temperature dependences of the susceptibility $\chi = M/H$ (Fig. 4) were measured in magnetic fields corresponding to the initial linear portions of the field dependences of the magnetization. For all the magnetic field orientations used in the measurements, the susceptibility varies only slightly with an increase in the temperature from 4.2 to 24 K and decreases drastically with a further increase in the temperature, which corresponds to a magnetic phase transition.

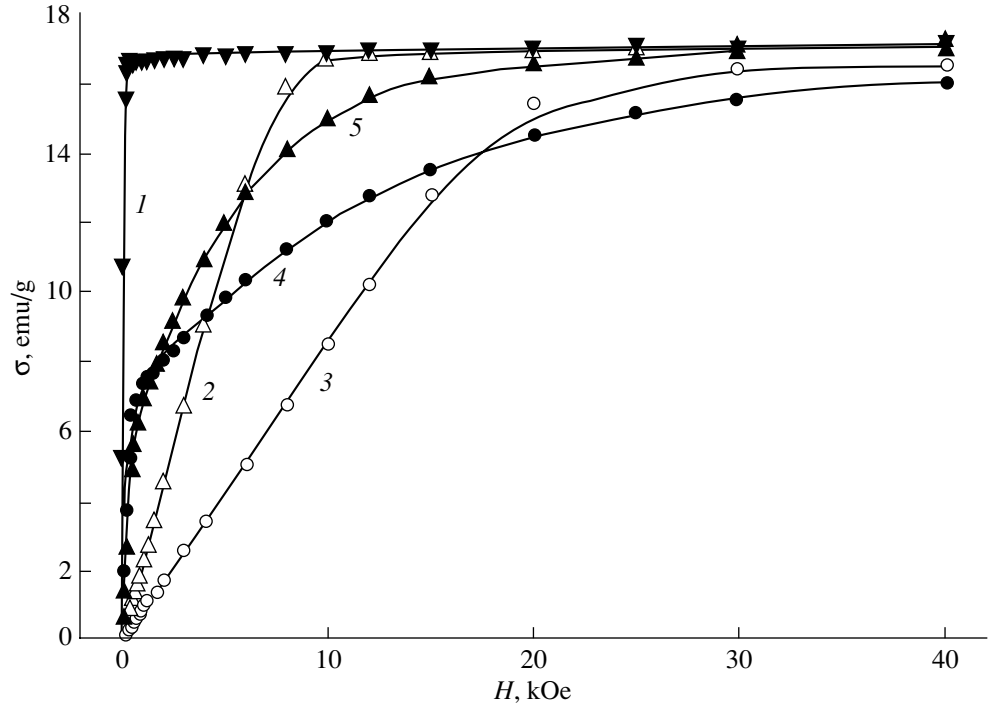

Fig. 3. Field dependences of the magnetization measured at $T = 5$ K. Curves *1–5* correspond to the magnetic field orientations *M*1–*M*5, respectively.

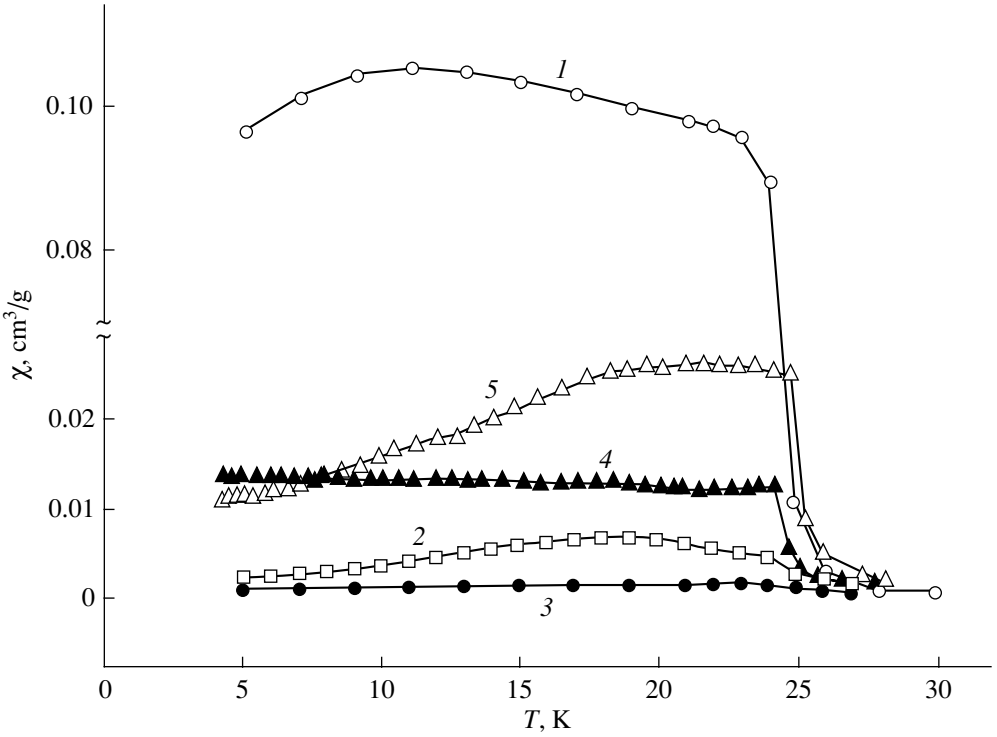

Fig. 4. Temperature dependences of the magnetic susceptibility for the $Cu_5Bi_2B_4O_{14}$ crystal at different orientations and strengths of the measuring field (Oe): (*1*) *M*1, 50; (*2*) *M*2, 500; (*3*) *M*3, 500; (*4*) *M*4, 20; and (*5*) *M*5, 20.

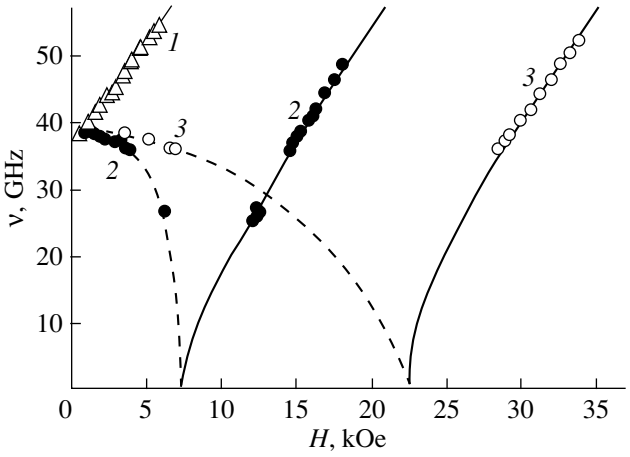

Fig. 5. Frequency–field dependences of the magnetic resonance measured at $T = 4.2$ K for different orientations of the external magnetic field: (*1*) $M1$, (*2*) $M2$, and (*3*) $M3$.

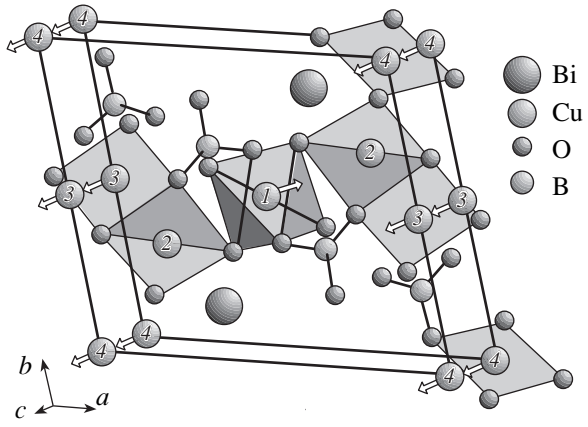

Fig. 6. Crystalline and hypothetical magnetic structures of $Cu_5Bi_2B_4O_{14}$.

The magnetic resonance measurements were performed on a pulsed magnetic spectrometer in the temperature range 4.2–80 K. The frequency–field dependences of the magnetic resonance measured at T = 4.2 K for the magnetic field orientations $M1$, $M2$, and $M3$ are plotted in Fig. 5. The frequency–field dependence at the orientation $M1$ exhibits a linear behavior and is characterized by an energy gap at approximately 36.5 GHz. For the other two orientations of the magnetic field, the frequency–field dependences can be divided into two portions. In weak fields, an increase in the magnetic field strength is accompanied by a decrease in the magnetic resonance frequency from a value determined by approximately the same energy gap as for the orientation $M1$. Then, beginning with a certain magnetic field, an increase in the magnetic field strength leads to an increase in the magnetic resonance frequency. The approximation of both portions in the frequency–field dependence of the magnetic resonance indicates that, for these two orientations of the magnetic field, the softening of the vibrational mode occurs at the same field strengths at which the magnetization reaches saturation.

4. DISCUSSION

The crystal structure of $Cu_5Bi_2B_4O_{14}$ is shown in Fig. 6. The unit cell contains one formula unit. The copper ions occupy four nonequivalent positions, which are designated as Cu(1)–Cu(4) (Fig. 6). The oxygen environment of each copper ion has the form of a distorted, strongly elongated octahedron (also depicted in this figure). The distances from the copper ion to the apical oxygen ions in the octahedron vary from 2.58 to 2.82 Å for different nonequivalent positions. Therefore, in order to evaluate the exchange interactions, it is sufficient to consider only the oxygen environment of the octahedron base in which the Cu–O distances for different positions lie in the range 1.78–2.08 Å. Note that, in this case, the octahedron base is not a regular square and the degree of its distortion differs for different nonequivalent positions.

Let us now consider the exchange interactions in terms of the Anderson–Goodenough–Kanamori theory [13]. It should be noted that all the exchange bonds allowed by the $Cu_5Bi_2B_4O_{14}$ structure occur through one oxygen ion; contrastingly, the exchange bonds in Bi_2CuO_4 [5] and CuB_2O_4 [9] occur through two oxygen ions and bismuth or boron ions. The crystal structure of $Cu_5Bi_2B_4O_{14}$ admits the formation of approximately 90° exchange bonds between the Cu(2) and Cu(3) ions, for which the base squares of the oxygen environment share a common side. There exists also an approximately 90° exchange bond between the Cu(2) and Cu(4) ions, for which the base squares of the oxygen environment share a common site. Moreover, the Cu(1) and Cu(2) ions are coupled by the exchange interaction through the oxygen ion located at a common site of their base squares. However, in the latter case, the bond angle θ is equal to 113.7°.

The estimation of the exchange integrals for these bonds according to the formulas taken from [13] gives

$$J_{23} = 4/3BCJ^{\text{int}} = +5\text{ K},$$
$$J_{24} = BCJ^{\text{int}} = +3\text{ K}, \quad (1)$$
$$J_{12} = 2B^2(U - 1/3J^{\text{int}})\cos\theta = -6.2\text{ K}.$$

Here, B is the parameter of the ligand–cation electron transfer over the σ bonds, C is the parameter of the ligand–cation electron transfer over the π bonds, J^{int} is the intraatomic-exchange integral, and U is the energy of oxygen–copper electron excitation. The above estimates were made using the standard parameters B = 0.02, C = 0.01, U = 2.2 eV, and J^{int} = 1.6 eV for Cu^{2+}

ions [14]. The paramagnetic Curie temperature Θ calculated in the molecular-field approximation using the exchange integrals obtained is equal to +3.6 K. This result is in qualitative agreement with the positive paramagnetic Curie temperature (Θ = +17.4 K), which was determined experimentally.

Reasoning from the results of analyzing the exchange interactions, we can propose the following magnetic structure of the $Cu_5Bi_2B_4O_{14}$ crystal (Fig. 6). The crystal has a ferrimagnetic structure consisting of two magnetic sublattices. In this structure, the Cu(1) ions belong to the first magnetic sublattice and all the other copper ions form the second magnetic sublattice. Judging from the proposed magnetic structure, the saturation magnetization can be estimated from the experimental effective magnetic moment $\mu_{eff} = 0.81\mu_B$, which was determined from the high-temperature portion of the temperature dependence of the magnetic susceptibility. The saturation magnetization thus calculated (σ = 7.6 emu/g) differs significantly from the experimental saturation magnetization (σ = 17.1 emu/g) obtained from the field dependences of the magnetization measured at T = 5 K (Fig. 3). Under the assumption that the proposed ferrimagnetic structure is incorrect and that the $Cu_5Bi_2B_4O_{14}$ crystal has a ferromagnetic structure, the saturation magnetization σ estimated from the same experimental effective magnetic moment is equal to 12.7 emu/g, which also differs substantially from the experimental value. However, we carried out the calculation for the proposed ferrimagnetic structure with the use of the effective magnetic moment $\mu_{eff} = 1.89\mu_B$, which is characteristic of copper ions. In this case, the effective magnetic moment was estimated from the experimental value g = 2.18. As a result, we obtained the saturation magnetization σ = 18.1 emu/g, which is close to the experimental value. Note that the reason for the considerable difference between the experimental and theoretical effective magnetic moments remains unclear.

The temperature of the magnetic phase transition can be most precisely determined from the experimental temperature dependence of the magnetization in the weak external magnetic field H = 20 Oe (Fig. 4). In this case, the true magnetization of the sample in the magnetic field ($m = \sigma + \chi H$) differs only slightly from the spontaneous magnetic moment σ. Therefore, it can be assumed that the drastic increase observed in the true magnetization at T = 24.5 K corresponds to a magnetic phase transition.

Thus, we believe that, at temperatures below T_C = 24.5 K, the $Cu_5Bi_2B_4O_{14}$ crystal is a collinear ferrimagnet.

Furthermore, the field dependences of the magnetization indicate that the ferrimagnetic structure of the studied crystal exhibits an easy-axis magnetic anisotropy with the easy axis aligned along the c axis of the crystal (the orientation $M1$). Since our attempts to determine the crystallographic indices of the small crystal face have been unsuccessful, we cannot argue that the orientations $M4$ and $M5$ coincide with the a and b axes of the crystal. However, the a axis is at least close to the directions $M3$ and $M4$ and the b axis is close to the directions $M2$ and $M5$. Hence, reasoning from the triclinic symmetry of the $Cu_5Bi_2B_4O_{14}$ crystal and the field dependences of the magnetization for the orientations $M2$–$M5$, we can assume that the a and b axes are the hard magnetic axes with saturation fields approximately equal to 25 and 10 kOe, respectively.

The initial linear portion in the field dependence of the magnetization at the orientation $M1$ is most likely associated with the domain structure of the crystal. The formation of a single-domain structure at this orientation is observed in a saturation field of 350 Oe. It can be assumed that the crystal has a predominantly strip domain structure with antiparallel orientations of the magnetic moments along the c axis in adjacent domains. Therefore, upon magnetization along the $M2$ and $M3$ directions perpendicular to the c axis, the initial portion of a rapid increase in the magnetization due to transformation of the domain structure is absent in the field dependences. For these orientations, an increase in the magnetic field strength immediately leads to rotation of the magnetic moments. Note that the magnetic moments of the adjacent domains rotate to meet each other toward the magnetic field direction and the domain structure is retained until the rotation ceases. For the magnetic field orientations $M4$ and $M5$, the projection of the magnetic field onto the c axis is nonzero and a rapid increase in the magnetization in the initial portions of the magnetization curves is caused by the displacement of the domain boundaries.

The above model of magnetic anisotropy in the $Cu_5Bi_2B_4O_{14}$ crystal is confirmed by the results of the magnetic resonance measurements. The magnetic resonance data are in qualitative agreement with the available data on the ferromagnetic resonance in a uniaxial ferromagnet [15]. The theoretical dependences constructed for the easy and hard magnetization directions under the assumption of a uniaxial ferromagnet are depicted by the solid lines in Fig. 5. Upon magnetization along the direction of easy magnetization, the frequency–field dependence exhibits a linear behavior and, in this specific case, can be described by the relationship [15]

$$\omega = \gamma(H_a' + H). \quad (2)$$

Note that the experimental data for the magnetic field orientation $M1$ are well represented by this formula at H_a' = 11.8 kOe and the gyromagnetic ratio γ = 3.05 MHz/Oe (the g factor is equal to 2.18). The parameter H_a' determines the energy gap in the magnetic resonance spectrum and, most likely, is a combination of the anisotropy fields for the a and b axes.

Upon magnetization along the $M2$ and $M3$ directions close to the hard magnetic axes b and a, the vibra-

tional frequencies in the initial portions of the frequency–field dependences decrease with an increase in the magnetic field strength. These portions correspond to a state in which the direction of the spontaneous magnetic moment does not coincide with the magnetic field direction and rotates gradually toward the latter direction with an increase in the field strength. The rotation is completed in a magnetic field equal to the anisotropy field in the corresponding direction. With a further increase in the magnetic field strength, the direction of the spontaneous magnetic moment coincides with the magnetic field direction. In this case, the frequency–field dependence can be represented in the following form [15]:

$$\omega = \gamma\{H(H - H_a)\}^{0.5}. \quad (3)$$

For both directions (*M*2 and *M*3), the experimental data in these portions of the frequency–field dependences are adequately described by relationship (3) at anisotropy fields H_{a1} = 7.5 kOe and H_{a2} = 22.5 kOe. These fields are close to the saturation fields determined for the orientations *M*2 and *M*3 from the magnetic measurements.

ACKNOWLEDGMENTS

This work was supported by the Russian Foundation for Basic Research, project no. 01-02-17270-a.

REFERENCES

1. A. Wells, *Structural Inorganic Chemistry* (Clarendon, Oxford, 1984; Mir, Moscow, 1987).
2. G. A. Petrakovskiĭ, K. A. Sablina, A. M. Vorotynov, *et al.*, Zh. Éksp. Teor. Fiz. **98** (4), 1382 (1990) [Sov. Phys. JETP **71**, 772 (1990)].
3. G. A. Petrakovskiĭ, Izv. Vyssh. Uchebn. Zaved., Fiz., No. 1, 91 (1998).
4. A. M. Vorotynov, A. I. Pankrats, G. A. Petrakovskiĭ, *et al.*, Zh. Éksp. Teor. Fiz. **113** (5), 1866 (1998) [JETP **86**, 1020 (1998)].
5. G. Petrakovskii, K. Sablina, A. Pankrats, *et al.*, J. Magn. Magn. Mater. **140–144**, 1991 (1995).
6. G. Petrakovskii, D. Velikanov, A. Vorotinov, *et al.*, J. Magn. Magn. Mater. **205** (1), 105 (1999).
7. A. I. Pankrats, G. A. Petrakovskiĭ, and N. V. Volkov, Fiz. Tverd. Tela (St. Petersburg) **42** (1), 93 (2000) [Phys. Solid State **42**, 96 (2000)].
8. G. A. Petrakovskiĭ, A. D. Balaev, and A. M. Vorotynov, Fiz. Tverd. Tela (St. Petersburg) **42** (2), 313 (2000) [Phys. Solid State **42**, 321 (2000)].
9. B. Roessli, J. Schefer, G. Petrakovskii, *et al.*, Phys. Rev. Lett. **86** (9), 1885 (2001).
10. M. I. Zargarov, N. M. Mustafaev, and N. S. Shuster, Neorg. Mater. **32** (1), 74 (1996).
11. F. Mizuno, H. Masuda, I. Hirobayashi, *et al.*, Nature **345** (7), 788 (1990).
12. M. A. Subramanian, A. P. Ramirez, and W. J. Marshall, Phys. Rev. Lett. **82** (7), 1558 (1999).
13. P. W. Anderson, Phys. Rev. **115** (1), 2 (1959); J. B. Goodenough, *Magnetism and the Chemical Bond* (Interscience, New York, 1963; Metallurgiya, Moscow, 1968).
14. O. A. Bayukov and A. F. Savitskiĭ, Fiz. Tverd. Tela (St. Petersburg) **36** (7), 1923 (1994) [Phys. Solid State **36**, 1049 (1994)].
15. A. G. Gurevich, *Magnetic Resonance in Ferrites and Antiferromagnets* (Nauka, Moscow, 1973).

Translated by O. Borovik-Romanova